



The behavior of the generated quantum correlations in two-SC-qubit system strongly coupled with a SC cavity in the presence of local noise

A.-B. A. Mohamed^{1,2} · M. Hashem²

Received: 22 January 2018 / Accepted: 12 July 2018 / Published online: 19 July 2018
© Springer Science+Business Media, LLC, part of Springer Nature 2018

Abstract

An analytical solution of the master equation that describes two charge superconducting qubits interacts with a single microwave cavity field mode within dispersive approximation and dissipation region of the qubit damping. Quantum correlations of a general two-qubit state (non-X-state) are studied by using three different quantum correlation quantifiers: measurement-induced non-locality, geometric quantum discord and logarithmic negativity. It is shown that the quantum correlations are sensitive to the choice of the parameters of the qubit dissipation rate, coherent state intensity and the initial qubit distribution angle. The generated oscillatory behavior of quantum correlations is different and more prominent as the noise rate decreases at the considered period of time.

Keywords Quantum correlations · Measurement-induced non-locality · Geometric quantum discord · SC qubits

1 Introduction

Quantum information is based on the realization of various forms of quantum correlations (QCs) including entanglement which is observed in composite systems. The existence of corrected states is essential for quantum information processing [1,2]; it has applications in quantum computing, quantum key distribution and quantum teleportation. Quantum entanglement (QE) is not the only kind of QCs that play an important role in quantum information and communication [2], but there are several measures of quantum correlations that have been presented [3–7]. Among these, quan-

✉ M. Hashem
mostafa_qbit@yahoo.com

¹ College of Science, Prince Sattam Bin Abdulaziz University, Al-Aflaj, Saudi Arabia

² Faculty of Science, Assiut University, Assiut, Egypt

tum discord (QD) [5,6] measures the QC between two partitions in a composite state. It is different from QE and may be nonzero even for certain separable states. QD is used to estimate the QCs in Grover search algorithm [10] and investigate the quantum phase transition [8,9]. Due to the difficult mathematical manipulation of the quantum discord, an explicit formula for the geometric quantum discord (GQD) [11] is presented by using the distance of Hilbert–Schmidt between two states: one of them is the given state, and the other one is the zero discord.

Another kind of QC is that results via the measurement-induced non-locality (MIN); it is defined as a dual to the GQD [4]. The MIN and the violation of Bell-type inequalities [2] are different ways to determine the non-locality in quantum states via the locally invariant measurements. If the non-locality of MIN is compared with the Bell non-locality (that is detected by violation of Bell-type inequalities), the MIN is a more general type of QCs based on the necessary disturbance induced by a local measurement. The MIN has many applications in quantum information, quantum cryptography [4], quantum dense coding [12] and remote state control [13]. The quantum correlations of bipartite quantum state have been studied in lots of previous results [14–16], while the models which have final X-state, the MIN and GQD have been widely studied in [17–21].

Research of the superconducting quantum circuits is now a flourishing field in quantum information processing. Thanks to their solid-state devices, they present an opportunity for building a quantum computer. The SC circuits have several different types of qubits: a charge qubit, [22,23], a phase qubit [22] and a flux qubit [22]. These types are currently the most experimentally advanced solid-state qubits. The charge qubit may be controlled flexibly through external tunable parameters, so it serves the quantum computation [24–27]. The strong coupling (dispersive limit) between a superconducting charge qubit and a coherent field has been experimentally observed [28–30]. The qubit-field interaction, in dispersive limit [30], is coherent and transfers the quantum information between the states of a SC qubit and cavity field. Recently, the strong coupling systems of a single photon in cavity field to a SC qubit have many potential applications in quantum information processing [31].

In practice, real quantum systems are unavoidably dissipated by their surrounding environments, where the interaction of a qubit-cavity system naturally involves two dissipative processes [32]: cavity damping and qubit spontaneous damping. This dissipation effect leads to deteriorate their quantum correlations. Therefore, it is extremely intriguing and important to investigate the dynamical behaviors of QCs in the dissipative quantum systems [33,34] and for X states [35–37]. Also, we consider the general two-qubit non-X-state by choosing the qubits which are initially in the superposition states to insure the final state of the two qubits has non-X-matrix. Compared with the previous studies, most prominent superiority of our paper is the computation of QCs for the density matrix of general two-qubit non-X-state. Consequently, we explore the difference between the quantum correlations in terms of MIN and GQD and quantum entanglement via the logarithmic negativity in a general state of two charge superconducting qubits in the dispersive approximation under a qubit damping.

This paper is structured as follows: In Sect. 2, the physical model and its solution are presented. In Sect. 3, a brief review of the quantum correlation measures is given.

Section 4 shows the computational results and discussions. Finally, we conclude our work in Sect. 5.

2 Driven superconducting model and its solution

Here, a real physical model consists of two charge qubits that are strongly coupled with a single-mode SC cavity. Each Cooper pair box of charge-qubit system contains a small superconducting island and two Josephson junctions. The circuits of the junctions contain the same Josephson energy E_J and capacitance C_J [38]. Each Cooper pair box is coupled to a gate voltage V_g via the gate capacitor C_g with the dimensionless gate charge $n_g = \frac{C_g V_g}{2e}$. Here our considerations are: (1) The classical magnetic field is switched to $\phi_c = \frac{1}{2}\phi_0$ with $n_g \neq \frac{1}{2}$. (2) The two approximations of rotating wave and dispersive regime are regarded. In the dispersive regime, the large detuning limit, there is not energy exchange between the charge-qubit systems and the microwave cavity field, is considered, i.e., $\delta = E_z - \omega \gg \frac{\pi|\eta_i|E_J}{\phi_0}\sqrt{\bar{n}}$ where \bar{n} is the mean photon numbers. Therefore, the dispersive Hamiltonian of the qubit-cavity system is given by [39]

$$\hat{H}_{\text{disp}} = \sum_{i=A,B} \frac{\pi^2|\eta_i|^2 E_J^2}{\delta\phi_0^2} \{ \hat{\sigma}_+^i \hat{\sigma}_-^i \hat{\psi} \hat{\psi}^\dagger - \hat{\sigma}_-^i \hat{\sigma}_+^i \hat{\psi}^\dagger \hat{\psi} + \hat{\sigma}_+^A \otimes \hat{\sigma}_-^B + \hat{\sigma}_-^A \otimes \hat{\sigma}_+^B \}, \quad (1)$$

where $\hat{\psi}^\dagger$ and $\hat{\psi}$ are the creation and annihilation operators of the SC-cavity field. The $\lambda = \frac{\pi^2|\eta_i|^2 E_J^2}{\delta\phi_0^2}$ is the dispersive coupling constant between the cavity field and the charge qubits. The parameters η_i have units of magnetic flux and depend on the SC cavity and the position of Cooper pair boxes. The third term describes the interaction between the charge qubits with flux quantum $\phi_0 = h/2e$. The charge energy E_z depends on the gate charge n_g . The operators $\hat{\sigma}_\pm^i$ are the usual Pauli matrices with the space spanned by the charge excited states, $|1\rangle_i$, and ground states, $|0\rangle_i$.

If we include the dissipation of SC-qubit spontaneous decay (qubit damping) in the Cooper pair boxes, the master equation that describes the time evolution of the qubit-cavity system is given by

$$\begin{aligned} \frac{d\hat{\rho}(t)}{dt} &= i[\hat{\rho}(t), \hat{H}_{\text{disp}}] \\ &+ \sum_{n=A,B} \gamma_n \left[2|0\rangle_{nn} \langle 1|\hat{\rho}(t)|1\rangle_{nn} \langle 0| - |1\rangle_{nn} \langle 1|\hat{\rho}(t) - \hat{\rho}(t)|1\rangle_{nn} \langle 1| \right], \quad (2) \end{aligned}$$

The γ_n ($n = A, B$) are the qubit dissipation rates; for simplicity, we take $\gamma_A = \gamma_B = \gamma$. To find the solution of the master equation of Eq. 2, we let the initial density matrix as:

$$\hat{\rho}(0) = \sum_{m,n=0} q_m q_n |m\rangle \langle n| \otimes \rho^{AB}(0), \quad (3)$$

where $q_n = e^{-\frac{|\alpha|^2}{2}} \frac{\alpha^n}{\sqrt{n!}}$. The SC-cavity field is initially prepared in coherent state $|\alpha\rangle\langle\alpha|$, where $|\alpha|$ is the coherent state intensity (mean photon numbers). While the two charge qubits are initially prepared in the superposition of the ground and excited states, i.e., $\hat{\rho}^{AB}(0) = |\phi\rangle\langle\phi|$, where $|\phi\rangle = \sin^2\theta|1\rangle + \sin\theta\cos\theta(|2\rangle + |3\rangle) + \cos^2\theta|4\rangle$.

In the bases $\{|1\rangle = |11\rangle, |2\rangle = |10\rangle, |3\rangle = |01\rangle, |4\rangle = |00\rangle\}$, the elements of the density matrix of the two charge qubits, $\hat{\rho}_{ij}(i, j = 1, 2, 3, 4)$, satisfy the following differential equation system:

$$\begin{aligned} \dot{\hat{\rho}}_{11} &= -2i\lambda \left[\hat{\psi}^\dagger \hat{\psi} \hat{\rho}_{11} - \hat{\rho}_{11} \hat{\psi}^\dagger \hat{\psi} \right] - 4\gamma \hat{\rho}_{11}, \\ \dot{\hat{\rho}}_{12} &= -i\lambda \left[2\hat{\psi}^\dagger \hat{\psi} \hat{\rho}_{12} + \hat{\rho}_{12} - \hat{\rho}_{13} \right] - 3\gamma \hat{\rho}_{12}, \\ \dot{\hat{\rho}}_{13} &= -i\lambda \left[2\hat{\psi}^\dagger \hat{\psi} \hat{\rho}_{13} + \hat{\rho}_{13} - \hat{\rho}_{12} \right] - 3\gamma \hat{\rho}_{13}, \\ \dot{\hat{\rho}}_{14} &= -2i\lambda \left[(1 + \hat{\psi}^\dagger \hat{\psi}) \hat{\rho}_{14} + \hat{\rho}_{14} \hat{\psi}^\dagger \hat{\psi} \right] - 2\gamma \hat{\rho}_{14}, \\ \dot{\hat{\rho}}_{22} &= -i\lambda \left[\hat{\rho}_{32} - \hat{\rho}_{23} \right] - 2\gamma \left[\hat{\rho}_{22} - \hat{\rho}_{11} \right], \\ \dot{\hat{\rho}}_{23} &= -i\lambda \left[\hat{\rho}_{33} - \hat{\rho}_{22} \right] - 2\gamma \hat{\rho}_{23}, \\ \dot{\hat{\rho}}_{24} &= -i\lambda \left[\hat{\rho}_{24}(1 + 2\hat{\psi}^\dagger \hat{\psi}) + \hat{\rho}_{34} \right] - \gamma \left[\hat{\rho}_{24} - 2\hat{\rho}_{13} \right], \\ \dot{\hat{\rho}}_{33} &= -i\lambda \left[\hat{\rho}_{23} - \hat{\rho}_{32} \right] + 2\gamma \left[\hat{\rho}_{11} - \hat{\rho}_{33} \right], \\ \dot{\hat{\rho}}_{34} &= -i\lambda \left[\hat{\rho}_{34}(1 + 2\hat{\psi}^\dagger \hat{\psi}) + \hat{\rho}_{24} \right] + \gamma \left[2\hat{\rho}_{12} - \hat{\rho}_{34} \right], \\ \dot{\hat{\rho}}_{44} &= 2i\lambda \left[\hat{\psi}^\dagger \hat{\psi} \hat{\rho}_{44} - \hat{\rho}_{44} \hat{\psi}^\dagger \hat{\psi} \right] + 2\gamma \left[\hat{\rho}_{11} + \hat{\rho}_{33} \right], \end{aligned} \tag{4}$$

and the rest elements verify: $\dot{\hat{\rho}}_{ij} = (\dot{\hat{\rho}}_{ji})^\dagger$.

By using Eq. 3, we can solve the above differential equation system. Therefore, the time evaluation of the two charge qubits is given by

$$\hat{\rho}^{AB}(t) = \sum_{m,n=1}^4 \rho_{mn} |m\rangle\langle n|, \tag{5}$$

where ρ_{mn} are the elements of the density matrix of $\hat{\rho}^{AB}(t)$, which are given by

$$\begin{aligned} \rho_{11} &= e^{-4\gamma t} \sin^4 \theta, \\ \rho_{12} = \rho_{13} &= \frac{1}{2} e^{-|\alpha|^2(1-e^{-2i\lambda t})-3\gamma t} \sin^2 \theta \sin 2\theta, \\ \rho_{14} &= \frac{1}{4} e^{-2\gamma t} \sin^2 2\theta e^{-2i\lambda t-|\alpha|^2(1-e^{-4i\lambda t})}, \\ \rho_{22} &= e^{-2\gamma t} [\cos^2 \theta - \sin^2 \theta (e^{-2\gamma t} - 1)] \sin^2 \theta, \\ \rho_{23} &= \frac{1}{2} e^{-2\gamma t} \sin^2 2\theta, \end{aligned}$$

$$\begin{aligned}
 \rho_{24} &= \frac{1}{2} e^{-|\alpha|^2(1-e^{-2i\lambda t})-\gamma t} \left[\frac{\gamma \sin^2 \theta \sin 2\theta}{i\lambda - \gamma} (e^{-2\gamma t} - e^{-2i\lambda t}) + \frac{1}{2} \sin 2\theta \cos \theta \right], \\
 \rho_{34} &= -\frac{1}{2} e^{-|\alpha|^2(1-e^{-2i\lambda t})-\gamma t} \left[\frac{\gamma \sin^2 \theta \sin 2\theta}{i\lambda - \gamma} (e^{-2\gamma t} - e^{-2i\lambda t}) + \frac{1}{2} \sin 2\theta \cos \theta \right], \\
 \rho_{44} &= \sin^4 \theta (e^{-2\gamma t} - 1)^2 - 2(e^{-2\gamma t} - 1) \sin^2 \theta \cos^2 \theta + \cos^4 \theta.
 \end{aligned} \tag{6}$$

In the following sections, we use the general two-qubit non-X-state, $\rho^{AB}(t)$, to discuss the effects of the qubit damping on some dynamical properties of the quantum correlations.

3 Quantum correlation measures

Here, we recall the definitions of the QC measures for a general quantum bipartite state, $\rho^{AB}(t)$, which expresses in terms of its Bloch representation and Pauli spin matrices σ_i as:

$$\hat{\rho}^{AB}(t) = \frac{1}{4} \left[I_{4 \times 4} + \sum_{i=1}^3 (x_i \sigma_i \otimes I_{2 \times 2} + I_{2 \times 2} \otimes y_i \sigma_i) + \sum_{ij=1}^3 r_{ij} \sigma_i \otimes \sigma_j \right], \tag{7}$$

where x_i and y_i are the components of the local Bloch vectors \vec{x} and \vec{y} , while $r_{ij} = \text{tr}\{\rho^{AB}(\sigma_i \otimes \sigma_j)\}$ are the components of the correlation matrix $R = [r_{ij}]$ [11]. If $\rho_{ij} = u_{ij} + i v_{ij}$ ($i, j = 1 - 4$) are the elements of ρ^{AB} , then the vector \vec{x} is given by

$$\vec{x} = (2u_{13} + 2u_{24}, 2v_{31} + 2v_{42}, 2\rho_{11} + 2\rho_{22} - 1)^t, \tag{8}$$

and the matrix R is given by

$$R = 2 \begin{pmatrix} u_{23} + u_{14} & v_{23} - v_{14} & u_{13} - u_{24} \\ v_{41} - v_{23} & u_{23} - u_{14} & v_{13} + v_{24} \\ u_{12} - u_{34} & v_{34} - v_{12} & \rho_{11} + \rho_{44} - \frac{1}{2} \end{pmatrix}. \tag{9}$$

By using the vector \vec{x} and the correlation matrix R , the GQD and MIN quantifiers are defined as the following:

- (i) Geometric quantum discord is given by [11]

$$G_t = \frac{1}{4} \left(\|\vec{x}\|^2 + \|R\|^2 - k_{\max} \right), \tag{10}$$

where the k_{\max} is the maximum eigenvalue of the matrix $K = \vec{x}\vec{x}^T + RR^T$. The GQD is used to quantify the quantum correlation via the minimum distance between the state, $\rho^{AB}(t)$ and a zero discord state.

(ii) Measurement-induced non-locality is defined by [4]

$$M_t = \begin{cases} \frac{1}{2} \left(\text{tr}RR^t - \frac{1}{\|\bar{x}\|} \bar{x}^t RR^t \bar{x} \right), & \bar{x} \neq 0; \\ \frac{1}{2} (\text{tr}RR^t - \mu_{\min}), & \bar{x} = 0. \end{cases}, \tag{11}$$

where μ_{\min} corresponds to the minimum eigenvalue of RR^t . From a geometric perspective, the MIN presents another type of QCs via the local von Neumann measurements from which one of the reduced states is left invariant.

(iii) Logarithmic negativity is defined by [40]

$$N_t = \log_2 \left[1 + 2 \sum_i |\mu_i| \right], \tag{12}$$

where $|\mu_i|$ are the absolute values of the negative eigenvalues of the partially transposed density matrix of $\hat{\rho}^{AB}(t)$. The logarithmic negativity is a good measure for quantum entanglement. It measures the QE of a final state $\hat{\rho}^{AB}(t)$ if it starts with pure state or mixed state.

4 Computational results

Figure 1 shows the influence of the distribution angle of the initial qubit states, θ , on the three QC quantifiers, where the M_t , G_t and N_t are depicted as functions of $\tau = \lambda t$ and $\theta \in [0, \pi]$, at the fixed value of $\gamma = 0$. At $\theta = 0.2\pi$ and $\tau = 0$ (before the interaction is started), we note that the initial values of the QC quantifiers are $M_{t=0} = G_{t=0} = N_{t=0} = 0$, i.e., the qubit states are uncorrelated. As soon as the interaction is started, the measures show that a highly correlated state can be generated, where the measurement-induced non-locality, the geometric quantum discord and the logarithmic negativity present different periodical behaviors with period π . They return to their initial values ($M_0 = G_0 = N_0 = 0$) at $\tau = n\pi$ ($n = 0, 1, 2, \dots$), to confirm that we plotted the dynamical behaviors of QC measures when $\tau \in [0, 2\pi]$ in Fig. 1c. In each period, the M_t grows and reaches its maximum value at $\tau = (2n - 1)\frac{\pi}{2}$, while the G_t and N_t reach twice to their maximum values in the same period. One can conclude that the charge qubits have three different types of QCs. Moreover, when looking at the θ -axis, $\theta \in [0, \pi]$, we find that the extreme values of M_t and N_t have periodic behavior (with respect to θ) with period $\theta = \frac{\pi}{2}$. This means that quantum correlations preserve their periodicity with the initial qubit distribution angle. The maximal values of M_t , G_t and N_t (where the two qubits have a maximum correlated state) for their peaks regularly appear at different values of τ and θ . It is clear that at the middle of each period $\tau = (n + 0.5)\pi$, ($n = 0, 1, 2, \dots$), the MIN and GQD have minimum value M_t^{\min} and maximal value G_t^{\max} at the same time, this emphasizes the fact that the MIN is a dual to the GQD. Therefore, we can deduce that the generated quantum correlations can be controlled by the initial qubit distribution angle.

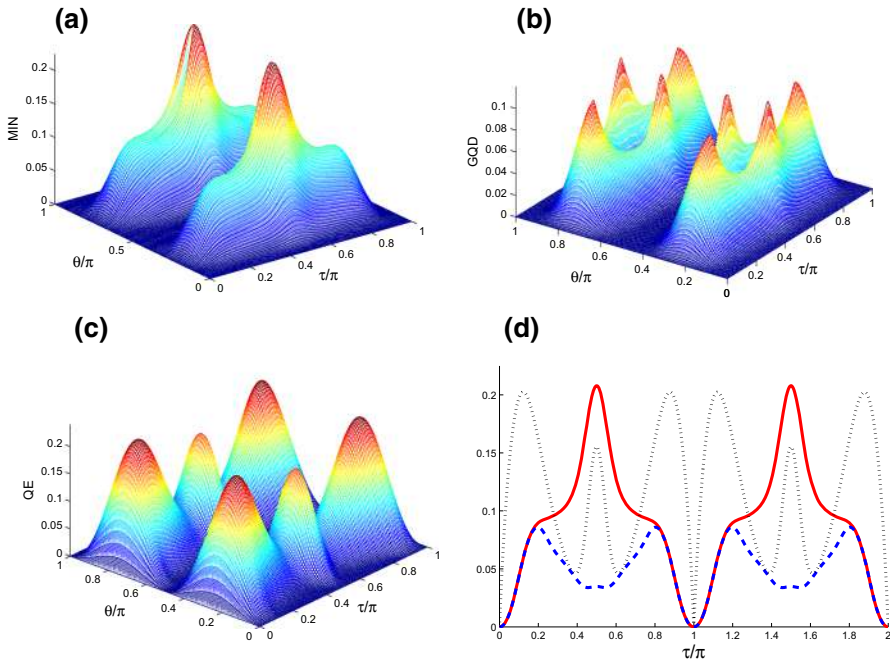


Fig. 1 Correlation measures, M_t in (a), G_t in (b) and N_t in (c) against interval used qubit distribution angle $\theta \in [0, \pi]$ and interval scaled time. **d** The M_t (solid curve), G_t (dashed curve) and N_t (dotted curve) are depicted for $\theta = 0.2\pi$. At fixed values of $\alpha = 1$ and $\gamma = 0$

In Fig. 2, we investigate the effect of the qubit dissipation rate γ/λ , where we set $\gamma \in [0, 0.2\lambda]$ with the fixed values of $|\alpha| = 1$ and $\theta = 0.2\pi$. At $\gamma = 0.1\lambda$ (see Fig. 2d), the M_t , G_t and N_t have the damped oscillatory behavior. After a long time, the states of the two SC qubits become separable (uncorrelated). In Fig. 2a–c, the qubit dissipation rate leads to decreasing the upper bounds of the quantum correlation measures. During the chosen interval of the qubit dissipation rate $\gamma \in [0, 0.2\lambda]$, the periodicity of the QCs is lost and their fluctuation develops as time decreases. These notable changes become more pronounced at large value of the γ/λ , where M_t , G_t and N_t completely may be vanished. This means that, for a certain value for the qubit dissipation rate, the generated quantum correlations of the two qubits disappeared (which are generated due to the interaction between the qubits and microwave cavity field). Finally, we find a competition between the interaction with and without the qubit damping parameter γ/λ , while the amplitudes of the QC quantifiers without the rate γ/λ are larger than those with it. The phenomena of the *sudden death* (correlated states drop abruptly to uncorrelated at a finite time [41,42]) and the *sudden birth* (i.e., the uncorrelated states grow suddenly at some finite time to be uncorrelated states [43]) appear clearly only for the logarithmic negativity.

In Fig. 3, the dependence of the QC measures, M_t , G_t and N_t on the initial coherent intensity, α , is displayed, where the M_t , G_t and N_t are depicted as Fig. 1 but with the large value of the initial coherent intensity $\alpha = 4$. By comparing the effects of the qubit

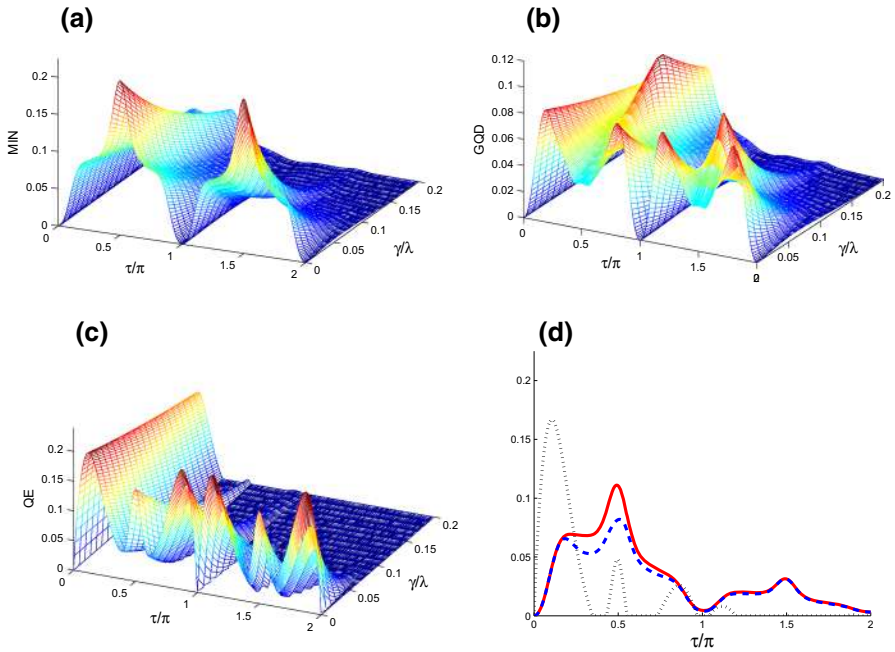


Fig. 2 Correlation measures, M_t in (a), G_t in (b) and N_t in (c) against interval used the qubit dissipation rate $\gamma \in [0, 0.2\lambda]$. Figure 2d is as Fig. 1d but for $\gamma = 0.1$, at fixed value of $\alpha = 1$

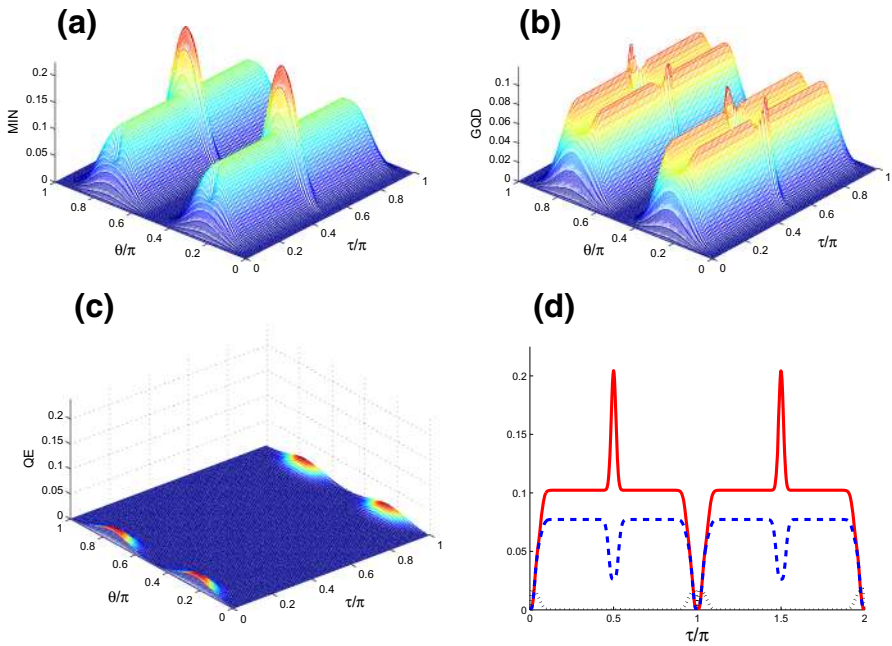


Fig. 3 As Fig. 1, but for $\alpha = 4$

distribution angle and the initial coherent intensity (see Figs. 1, 3) on the dynamical behavior of the quantum correlations, we find notable changes. We can deduce that the M_t , G_t and N_t are very sensitive not only to the qubit distribution angle as mentioned before but also to the initial coherent intensity. From Figs. 1 and 3, we observe that M_t , G_t are more robust than N_t , where the M_t and G_t may be strengthened by increasing the initial coherent intensity, whereas the logarithmic negativity weakens. The increase in the initial coherent intensity leads to increasing and sharpening the peaks of the M_t and G_t . Moreover, its maximum and minimum values are more maintenance. In Fig. 3c, we can see some revival of small peaks for the logarithmic negativity, which appear as a series and disappears as the initial coherent intensity increases. From Fig. 3d, we observe that the M_t and G_t have nonzero values and reach their maximum values in the same time intervals of the death entanglement intervals. But when the logarithmic negativity reaches its maximum values, M_t and G_t return to their initial zero values. Therefore, we may deduce that the measurement-induced non-locality, the geometric quantum discord and the logarithmic negativity present different quantum correlations in the considered system, and the QE is not only a type of quantum correlations but there are separable states which may have other types for the quantum correlations as MIN and GQD.

In Fig. 4, the combined effects of the qubit dissipation rate γ/λ and the initial coherent intensity, α , on the QCs of $\hat{\rho}^{AB}(t)$ are displayed. We observe that the amplitudes of the QC functions decrease under the influence of the qubit dissipation rate γ/λ . The threshold time for the death of the measures depends on the initial coherent intensity and the qubit dissipation rate. A remarkable property of the initial coherent intensity α with the qubit damping consists in the fact that the QCs can fall to zero value and remains nearly invariant regardless of the increase in the λt , i.e., the state of the two charge qubits, $\rho^{AB}(t)$, becomes separable.

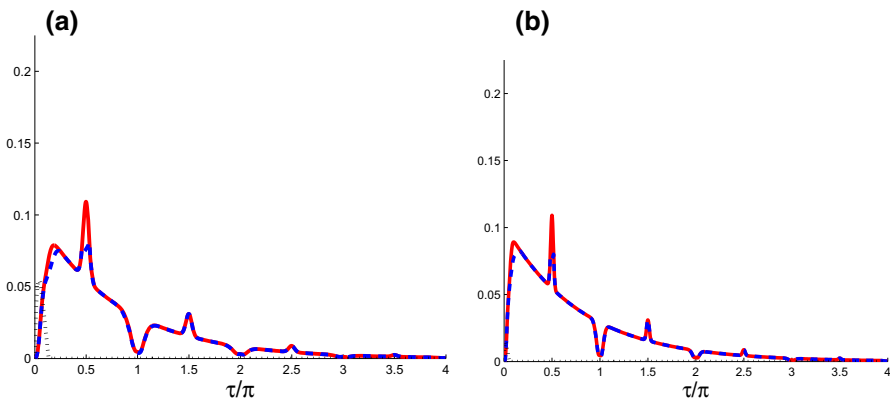


Fig. 4 Time evolutions of M_t (solid curve), G_t (dashed curve) and N_t (dashed dotted curve) for $\alpha = 2$ in (a) and $\alpha = 4$ in (b) at fixed values for $\theta = 0.2\pi$ and $\gamma = 0.1\lambda$

5 Conclusion

An analytical solution for a system consists of two-charge-qubit system in a SC cavity with full wavelength which is introduced in the dispersive regime. The QCs via the measurement-induced non-locality and geometric quantum discord are compared with QE via the logarithmic negativity under the influence of the qubit damping. The SC cavity is initially prepared in coherent states, and the two SC qubits are initially prepared in superposition states. When the effect of the qubit dissipation rate is neglected, one can find that M_t , G_t and N_t do not have the same behavior, i.e., both the M_t and G_t present a new quantum correlations unlike that is presented by N_t . It is found that the generation of correlations depends not only on the initial states but also on the dissipation of the qubit decay, where the qubit dissipation rate destroys the generated quantum correlations. By increasing the initial coherent intensity and the qubit decay, the QCs can fall to zero value for a very long time and will not be recovered, i.e., the state of the two SC qubits becomes separable. The QE is not only a kind of quantum correlations in two-charge-qubit system, but it is found that some separable two charge qubits, $N_t = 0$, may possess other quantum correlations via MIN and GQD.

Acknowledgements The authors would like to thank the reviewers for their subjective comments that helped to improve the manuscript.

References

- Masanes, L.: All bipartite entangled states are useful for information processing. *Phys. Rev. Lett.* **96**, 150501 (2006)
- Nielsen, M.A., Chuang, I.L.: *Quantum Computation and Quantum Information*. Cambridge University Press, Cambridge (2000)
- Luo, S.: Using measurement-induced disturbance to characterize correlations as classical or quantum. *Phys. Rev. A* **77**, 022301 (2008)
- Luo, S., Fu, S.: Measurement-induced nonlocality. *Phys. Rev. Lett.* **106**, 120401 (2011)
- Ollivier, H., Zurek, W.H.: Quantum discord: a measure of the quantumness of correlations. *Phys. Rev. Lett.* **88**, 017901 (2001)
- Henderson, L., Vedral, V.: Classical quantum and total correlations. *J. Phys. A* **34**, 6899 (2001)
- Mohamed, A.-B.A., Eleuch, H.: Generation and robustness of bipartite non-classical correlations in two nonlinear microcavities coupled by an optical fiber. *J. Opt. Soc. Am. B* **35**, 47–53 (2018)
- Dillenschneider, R.: Quantum discord and quantum phase transition in spin chains. *Phys. Rev. B* **78**, 224413 (2008)
- Sarandy, M.S.: Classical correlation and quantum discord in critical systems. *Phys. Rev. A* **80**, 022108 (2009)
- Cui, J., Fan, H.: Correlations in the Grover search. *J. Phys. A Math. Theor.* **43**, 045305 (2010)
- Dakic, B., Vedral, V., Brukner, C.: Necessary and sufficient condition for nonzero quantum discord. *Phys. Rev. Lett.* **105**, 190502 (2010)
- Li, X., Pan, Q., Jing, J., Zhang, J., Xie, C., Peng, K.: Quantum dense coding exploiting a bright Einstein-Podolsky-Rosen beam. *Phys. Rev. Lett.* **88**, 047904 (2002)
- Bennett, C.H., DiVincenzo, D.P., Shor, P.W., Smolin, J.A., Terhal, B.M., Wootters, W.K.: Remote state preparation. *Phys. Rev. Lett.* **87**, 077902 (2001)
- Shi, J.-D., Wang, D., Ye, L.: Comparative explorations of the revival and robustness for quantum dynamics under decoherence channels. *Quantum Inf. Process.* **15**, 1649–1659 (2016)
- Shi, J.D., Wang, D., Ma, W.C., Ye, L.: Enhancing quantum correlation in open-system dynamics by reliable quantum operations. *Quantum Inf. Process.* **14**, 3569–3579 (2015)

16. Mohamed, A.-B.A.: Pairwise quantum correlations of a three-qubit XY chain with phase decoherence. *Quantum Inf. Process.* **12**, 11411153 (2013)
17. Wu, S.-X., Zhang, J., Yu, C.-S., Song, H.-S.: Uncertainty-induced quantum nonlocality. *Phys. Lett. A* **378**, 344 (2014)
18. Mohamed, A.-B.A., Joshi, A., Hassan, S.S.: Bipartite non-local correlations in a double-quantum-dot excitonic system. *J. Phys. A Math. Theor.* **47**, 335301 (2014)
19. Obada, A.-S.F., Mohamed, A.-B.A.: Quantum correlations of two non-interacting ion's internal electronic states with intrinsic decoherence. *Opt. Commun.* **309**, 236 (2013)
20. Tian, Z., Jing, J.: Measurement-induced-nonlocality via the Unruh effect. *Ann. Phys.* **333**, 76 (2013)
21. Wei, J.-L., Li, X.-L., Zhang, X.-Z., Guo, J.-L.: Dynamical behavior of quantum correlations between two qubits coupled to an external environment. *Quantum Inf. Process.* **15**, 24252440 (2016)
22. You, J.Q., Nori, F.: Superconducting circuits and quantum information. *Phys. Today* **58**, 42 (2005)
23. You, J.Q., Tsai, J.S., Nori, F.: Controllable manipulation and entanglement of macroscopic quantum states in coupled charge qubits. *Phys. Rev. B* **68**, 024510 (2003)
24. Niskanen, A.O., Harrabi, K., Yoshihara, F., Nakamura, Y., Lloyd, S., Tsai, J.S.: Quantum coherent tunable coupling of superconducting qubits. *Science* **316**, 723 (2007)
25. Obada, A.-S.F., Hessian, H.A., Mohamed, A.-B.A., Homid, A.H.: A proposal for the realization of universal quantum gates via superconducting qubits inside a cavity. *Ann. Phys.* **334**, 47 (2013)
26. You, J.Q., Tsai, J.S., Nori, F.: Hybridized solid-state qubit in the charge-flux regime. *Phys. Rev. B* **73**, 014510 (2006)
27. Obada, A.-S.F., Hessian, H.A., Mohamed, A.-B.A., Homid, A.H.: Efficient protocol of N -bit discrete quantum Fourier transform via transmon qubits coupled to a resonator. *Quantum Inf. Process.* **13**, 475 (2014)
28. Wallraff, A., Schuster, D.I., Blais, A., Frunzio, L., Huang, R.-S., Majer, J., Kumar, S., Girvin, S.M., Schoelkopf, R.J.: Strong coupling of a single photon to a superconducting qubit using circuit quantum electrodynamics. *Nature* **431**, 1627 (2004)
29. Reithmaier, J.P., Löffler, A., Sk, G., Hofmann, C., Kuhn, S., Reitzenstein, S., Keldysh, L.V., Kulakovskii, V.D., Reinecke, T.L., Forchel, A.: Strong coupling in a single quantum dot-semiconductor microcavity system. *Nature* **432**, 197 (2004)
30. Mabuchi, H., Doherty, A.C.: Cavity quantum electrodynamics: coherence in context. *Science* **298**, 1372 (2002)
31. Orgiazzi, J.-L., Deng, C., Layden, D., Marchildon, R., Kitapli, F., Shen, F., Bal, M., Ong, F., Lupascu, A.: Flux qubits in a planar circuit quantum electrodynamics architecture: quantum control and decoherence. *Phys. Rev. B* **93**, 104518 (2016)
32. Blais, A., Huang, R.-S., Wallraff, A., Girvin, S.M., Schoelkopf, R.J.: Cavity quantum electrodynamics for superconducting electrical circuits: an architecture for quantum computation. *Phys. Rev. A* **69**, 062320 (2004)
33. Shi, J.-D., Xu, S., Ma, W.-C., Song, X.-K., Ye, L.: Purifying two-qubit entanglement in nonidentical decoherence by employing weak measurements. *Quantum Inf. Process.* **14**, 1387–1397 (2015)
34. Shi, J.D., Wu, T., Song, X.K., Ye, L.: Dynamics of entanglement under decoherence in noninertial frames. *Chin. Phys. B* **23**, 020310 (2014)
35. Ann, K., Jaeger, G.: Finite-time destruction of entanglement and non-locality by environmental influences. *Found. Phys.* **39**, 790 (2009)
36. Bellomo, B., Compagno, G., Lo Franco, R., Ridolfo, A., Savasta, S.: Dynamics and extraction of quantum discord in a multipartite open system. *Int. J. Quantum Inf.* **9**, 1665 (2011)
37. Shi, J.D., Wu, T., Song, X.K., Ye, L.: Multipartite concurrence for X states under decoherence. *Quantum Inf. Process.* **13**, 1045–1056 (2014)
38. Makhlin, Y., Schön, G., Shnirman, A.: Josephson-junction qubits with controlled couplings. *Nature* **398**, 305 (1999)
39. Liu, Y.-X., Wei, L.F., Nori, F.: Measuring the quality factor of a microwave cavity using superconducting qubit devices. *Phys. Rev. A* **72**, 033818 (2005)
40. Vidal, G., Werner, R.F.: Computable measure of entanglement. *Phys. Rev. A* **65**, 032314 (2002)
41. Yu, T., Eberly, J.H.: Finite-time disentanglement via spontaneous emission. *Phys. Rev. Lett.* **93**, 140404 (2004)
42. Mohamed, A.-B.A., Hessian, H.A., Obada, A.-S.F.: Entanglement sudden death of a SC-qubit strongly coupled with a quantized mode of a lossy cavity. *Physica A* **390**, 519 (2011)
43. Ficek, Z., Tanaś, R.: Delayed sudden birth of entanglement. *Phys. Rev. A* **77**, 0543011 (2008)